

International Conference on Space Optics—ICSO 2018

Chania, Greece

9–12 October 2018

Edited by Zoran Sodnik, Nikos Karafolas, and Bruno Cugny



NanoCarb part 1: compact snapshot imaging interferometer for CO₂ monitoring from space

Yann Ferrec

Guillaume Bonnery

Laure Brooker

Laurence Croizé

et al.



icso proceedings



NanoCarb part 1: Compact snapshot imaging interferometer for CO2 monitoring from space

Yann Ferrec^{*a}, Guillaume Bonnery^b, Laure Brooker^b, Laurence Croizé^a, Silvère Gousset^c, Etienne Le Coarer^c, and the SCARBO consortium^d

^aONERA/DOTA, BP 80100, chemin de la Hunière, 91123 Palaiseau, France;

^bAirbus Defence and Space, 31, rue des Cosmonautes, 31402 Toulouse, France ;

^cInstitut de Planétologie et d'Astrophysique de Grenoble, Université Grenoble-Alpes, 38058 Grenoble, France ;

^d<http://scarbo-h2020.eu/>

ABSTRACT

Nanocarb is a snapshot imaging interferometer concept dedicated to the measurement of CO₂. Thanks to its very compact design, it is a good candidate for small satellites, which would pave the way to a constellation of satellites to monitor emission of anthropogenic greenhouse gases from space. Nanocarb is based on a multiaperture design, with a stepcase interferometric plate to measure partial interferograms. It is developed in the framework of the Scarbo project, an European project involving several partners, the aim of which being to design and analyse the performances of the Nanocarb concept, complemented by collocated compact aerosol sensor and CO₂ reference instruments. The overall measurement concept will be experimentally validated through a dedicated airborne campaign featuring instrument prototypes.

Keywords: Air pollution monitoring, Anthropogenic GHG emissions, Fabry-Perot, Fourier transform spectroscopy, Optical instrumentation, Passive remote sensing

1. INTRODUCTION

There are currently several satellites dedicated to the passive monitoring of greenhouse gases (GHG) like CO₂ or CH₄ from space: for instance GOSAT¹, OCO-2², or GHGSat³. Next missions include Microcarb⁴ or CarbonSat⁵. Nevertheless, all these missions lack the temporal resolution needed to measure diurnal changes of GHG emissions over large or scattered areas of interest. The *Space CARBOn Observatory* (SCARBO) is a Horizon 2020 project, aiming at designing a system for the monitoring of anthropogenic emissions of CO₂ with a daily and global revisit of the Earth for an affordable cost (see Table 1). This project, which began December 2017 for 3 years, is implemented by a consortium of 10 European organizations, and includes instrumental developments and high level data processing for the science data retrieval chain. The Scarbo mission concept is to deploy a constellation of small satellites embarking miniaturised GHG sensors coupled with aerosols sensors for the improvement of the measurement accuracy. This constellation will adequately complement the low-revisit high-performance satellites.

Table 1. Operational mission needs for a future operational GHG monitoring system.

global coverage	weekly
footprint	few km
revisit	<12h
CO ₂ concentration resolution	1 ppm

With such a constellation of small satellites, the payload has to be very compact. This is why one of the main components of Scarbo is Nanocarb⁶, a compact imaging interferometer (see Section 2) dedicated to GHG measurement. The NanoCarb concept may represent a breakthrough in terms of size, mass and power. It is based on two main features:

- it uses a very compact static imaging interferometer;
- it measures only a partial interferogram.

The measurement of only a partial interferogram allows to improve both spatial coverage and spectral resolution. Indeed, measuring only the most informative part of the interferogram leads to an efficient use of the available observation time and the number of pixels, making way to snapshot spectral imaging. Regarding the interferometer, the use of a low finesse Fabry-Perot filter reduces the size of the device, by eliminating the need of a beam-splitter.

These two ideas are combined in the NanoCarb concept through a lenslet array: the interferometric plate has a stepcase shape, so that in front of each microlens there is a parallel plate with a fixed thickness, and consequently a fixed optical path difference. Thus, we obtain a set of small images of the same scene on the focal plane array (FPA), each associated with a different OPD. After image registration, we can retrieve the partial interferogram for each ground point (see Figure 1).

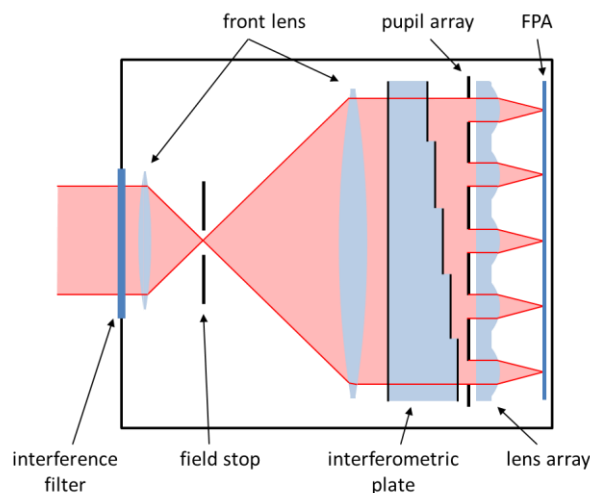


Figure 1. Optical principle of Nanocar: a front afocal lens with a field stop is located before the core of Nanocar, consisting in the interferometric plate and the lens array. Light is then focused on the FPA to obtain a set of images, each one being associated to one thickness of the interferometric plate.

To validate the performance of such an instrument, a first prototype will be developed within the framework of Scarbo project (see Section 3.). This prototype will be designed for an airborne campaign which will occur at the end of the project. During this campaign, three instruments will be deployed: Nanocar, but also Spex⁷, an instrument developed by SRON to measure aerosol, and Mamap⁸, our reference instrument for airborne CO₂ measurement developed by the University of Bremen.

2. THE NANOCARB CONCEPT

As stated above, the Nanocar concept has two main features: measuring only partial interferograms, through a low finesse Fabry Perot interferometer. We detail these two aspects below.

2.1 Partial interferograms

The goal is not here to perform a detailed analysis of CO₂ concentration retrieval from space, but to heuristically explain the principle of partial interferograms. The gist of this method can be seen on Figure 2: the spectral signature of CO₂ is close to a periodic signal around 6200 cm⁻¹. Therefore, in the Fourier space of the spectrum (that is, in the interferogram space), most of information on CO₂ is concentrated at few optical path differences (OPD), here around 5.5 mm. Consequently, if we are limited to the measurement of only few tens of points in the interferogram (for snapshot spectral imaging), the most efficient way to acquire information on CO₂ is to acquire the interferogram only around this OPD.

The acquisition of partial interferograms is not a new idea: it was already developed in the 1970s by Kyle for temperature measurement through CO₂ lines⁹ and by Fortunato who applied this method to the measurement of SO₂ concentration¹⁰. It was more recently studied for instance by Pierangelo for the SIFTI instrument¹¹ and by Grieco for IASI data processing¹². However, the feature of Nanocar is that the spectral band is purposely limited for such a partial interferogram, with a trade-off on the position and width of the spectral band versus the useful signal to noise ratio, which means that useless information (with respect to CO₂) is both optically filtered in the spectral domain and in the

Fourier domain. Nevertheless, despite this filtering, interferent species like water can disturb the CO₂ retrieval: that is why, on Nanocarb, the choice of the OPD will be done taking into account these effects (see Figure 3). More details about the processing of Nanocarb partial interferograms can be found in another proceeding¹⁴.

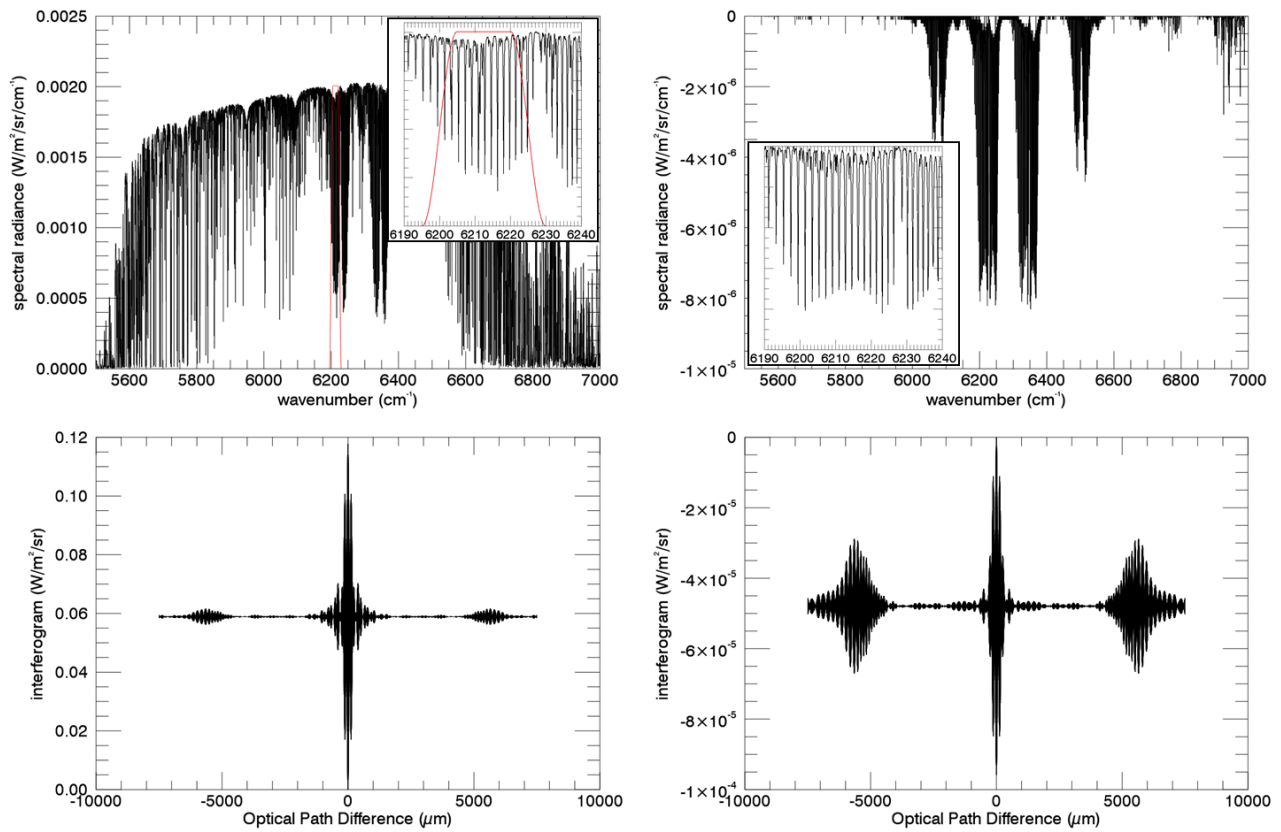


Figure 2. Typical radiance simulated with Modtran for a spaceborne mission viewing at nadir. Top: spectra; bottom: corresponding interferograms after filtering between 6200 cm⁻¹ and 6225 cm⁻¹ (red curve). Left: total radiance with a CO₂ concentration of 400 ppm; right: difference between the radiance with 405 ppm and with 400 ppm of CO₂, the other parameters being unchanged.

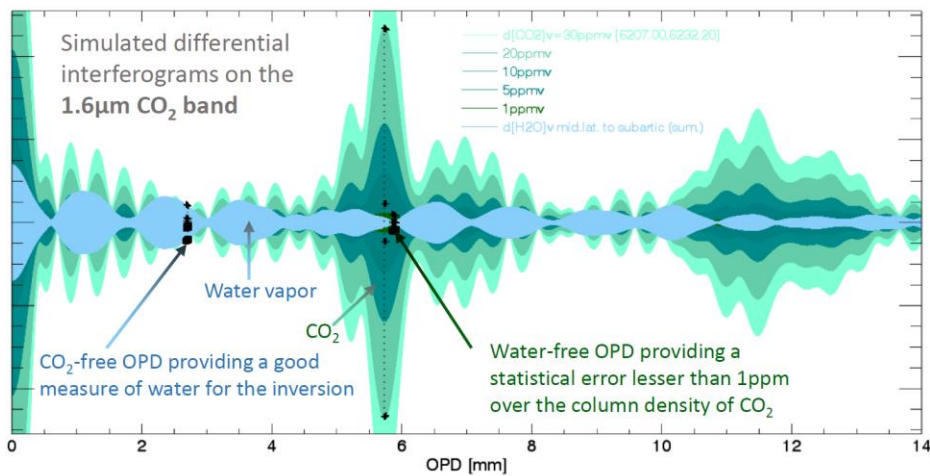


Figure 3. Jacobian interferograms (arbitrary unit) when varying the CO₂ or H₂O concentration¹³. During the design phase of Nanocarb, the choice of the measured OPD will be done taking into account the impact of other species than CO₂.

2.2 Nanocarb interferometer

In order to have a very compact and stable interferometer, we have chosen to use a Fabry-Perot interferometer, but with a low finesse, so that it is close to a two-wave interferometer^{15,16,17,18} (see Figure 4).

This solution is indeed advantageous because, by eliminating the beamsplitter, this interferometer is extremely compact, being also very thin. Besides, this static interferometer can be made monolithic, and consequently cannot be detuned; the only source of error may come from thermal variation, but thanks its compactness, Nanocarb (interferometric plate, lens array, and FPA) can be quite easily thermally regulated, if not integrated in the cryogenic dewar of the FPA. Lastly, the use of only partial interferograms solves the issue of measuring very low OPD which may be quite difficult for a Fabry Perot interferometer.

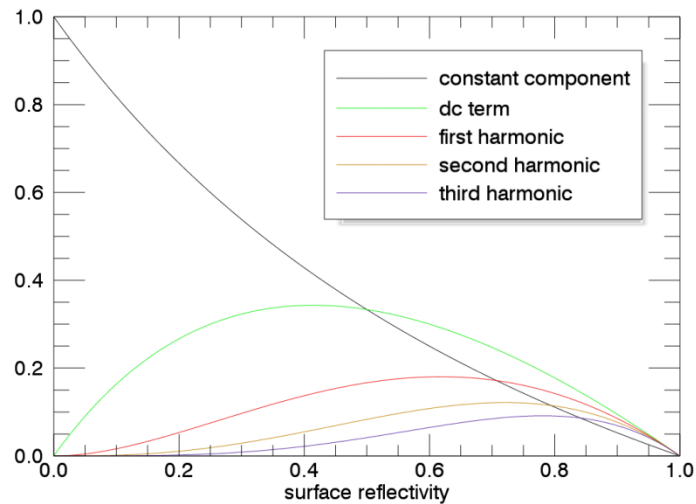


Figure 4. Amplitude of the Fourier components for a Fabry Perot interferometer, vs the reflectivity of the surfaces of the cavity. In a two-wave interferometer, there would be only the dc term and the fundamental frequency: we can see that for reflectivity about 30%, the Fabry-Perot interferometer is close to a two-wave interferometer, with a transmission about 55% and an intrinsic fringe contrast of 60%.

On the other hand, the main difficulty generated by the design of Nanocarb is the chessboard shape of the interferometric plate. The plate could be manufactured in one piece of material ("glass" cavity), or made by the assembly of two external plates ("air" cavity); moreover, the steps can be engraved on only one side, or on the two sides with unidimensional steps (see Figure 5).

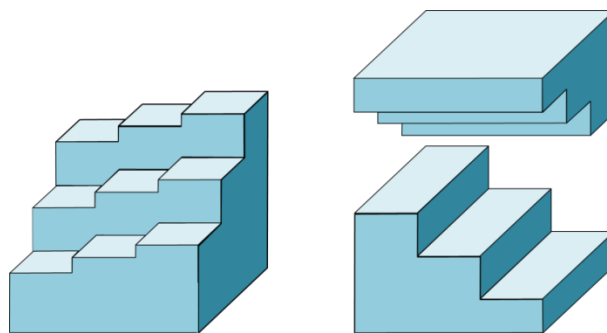


Figure 5. Two examples of possible geometry for the interferometric plate. On the left, it is made inside one material, with only one side engraved with a two-dimensional pattern. On the right, the cavity is formed between the inner sides of two plates each engraved with a one-dimensional pattern.

Currently, our choice for Nanocarb is to manufacture the plate in a monolithic piece of Silicon¹⁹. This choice has two benefits due to the high index of Silicon ($n_{Si} = 3.4$). Firstly, without any coating on the surfaces, the Fresnel reflection coefficient is equal to 30%, that to say in the optimal range defined above (see Figure 4). Secondly, a high refractive index significantly improves the angular acceptance inside the plate, which in turns allows to widen the entrance pupil

and to increase the field-of-view. Indeed, two phenomena have to be considered. The first one is the filtering of the annular fringes by the finite size of the pixel: in an interferometer with flat and parallel mirrors (so without field widening), the OPD depends on the angle inside the cavity in accordance with Equation (1).

$$OPD = 2ne \cos \theta \quad (1)$$

with n and e the refractive index and the thickness of the cavity, and θ the angle *inside the cavity* (with respect to the normal to the mirrors). This leads to the well-known Haidinger fringes, imaged in the plane of the FPA by the lens. Due to its finite size, one pixel sees several angles, thus several OPD, which decreases the contrast of the measured fringes, especially for high angles of view where the fringe spacing is lower. Let us note FOV the maximal field-of-view and $IFOV$ the angular size of one pixel, *outside the cavity*. If we decide that inside $IFOV$, the OPD must not vary more than $\lambda/4$, with λ the wavelength of the light in the vacuum, then we obtain an upper limit on FOV :

$$FOV < \lambda \cdot n^2 / 4OPD_{max} \cdot IFOV \quad (2)$$

A high refractive index n thus allows to increase the field-of-view without blurring the detected fringes.

The second benefit of a high index is to limit the crosstalk between the small images. Indeed, there are currently no walls inside the interferometric plate to separate the steps. Therefore, we must take care that the light reflected in the cavity does not intercept the neighbouring step (see Figure 6). Very roughly, a necessary condition to avoid this effect is given by Equation (3):

$$FOV < (\phi_{tot} - \phi_{pupil}) \cdot n^2 / 2OPD_{max} \quad (3)$$

where ϕ_{tot} is the diameter of one small image and ϕ_{pupil} is the diameter of one pupil. A high refractive index n thus allows either to increase the field-of-view, or -if the maximal field-of-view is already reached- to increase the pupil diameter.

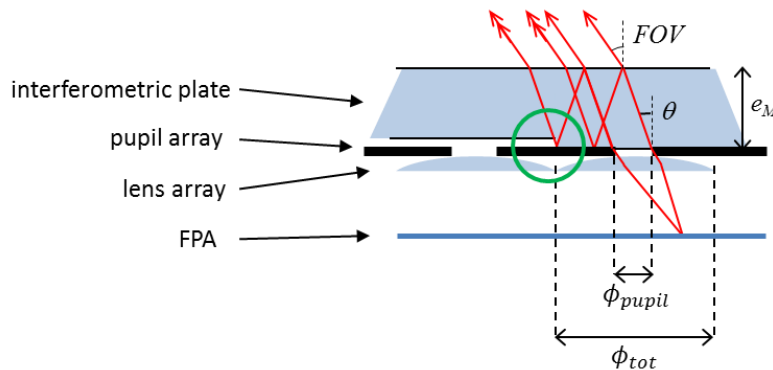


Figure 6. Upper limit for the field-of-view before cross-talk between two contiguous steps. In red, we have drawn rays from the FPA toward the scene. If we increase the field-of-view, then the marginal ray after one round-trip will be reflected by the neighbouring step (emphasized by the green circle).

3. THE SCARBO PROJECT

For now, Nanocarb is mainly a concept and has to be technologically developed (both hardware and software) and experimentally demonstrated. However, Nanocarb alone is not sufficient for a space mission aiming at monitoring GHG emissions, and a more global view is needed. This is the ambition of the Scarbo project: to demonstrate the feasibility of an innovative GHG miniaturised sensor to assess the potential of an operational mission concept, based on a constellation of complementary space sensors measuring GHG anthropogenic emissions for commercial and institutional applications (see Figure 7). To reach this objective, works will be led in complementary directions, taking advantages of the various skills of the Scarbo partners: Airbus (France, Germany and Netherlands), LMD/CNRS (France), Noveltis (France), Onera (France), SpaceTech (Belgium), SRON (Netherlands), Universität Bremen (Germany), Université Grenoble-Alpes (France).

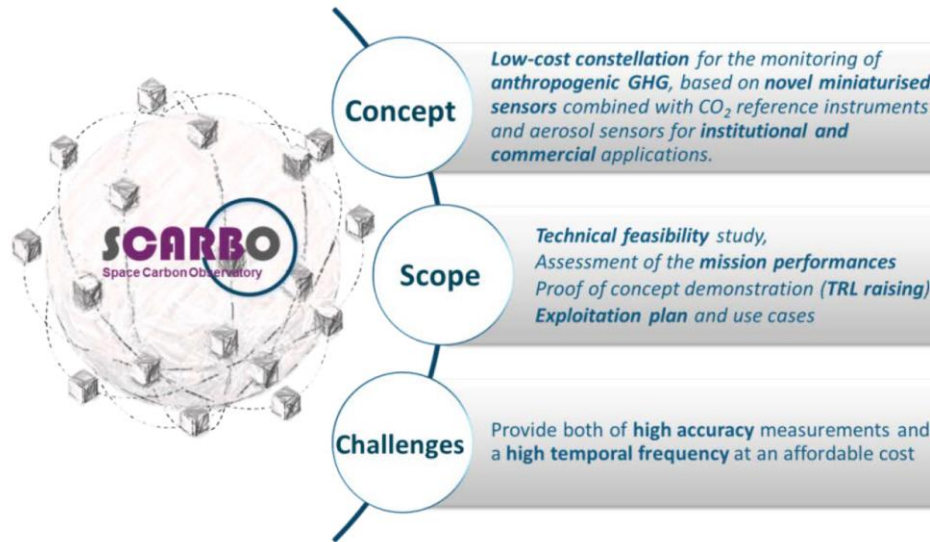


Figure 7. Summary of Scarbo general outline. The Scarbo mission and sensors concept, based on novel technological developments maturation, would allow for an operational implementation by 2030.

Three main parts can be identified in the Scarbo project: analysis of a space mission, instrumental developments, and experimental demonstration through an airborne campaign.

3.1 Requirements for a space mission

The definition of a mission requirements starts with the user needs collection, in order to have appropriate elements for making well-informed choices and prioritizations. These user needs are about CO₂ and CH₄ fluxes, that is about products of level L4 (see Figure 8). They have therefore to be translated to requirements on the L2 products, that is on the precision and accuracy of CO₂ and CH₄ concentration, and to spatio-temporal sampling and resolution characteristics. This will be performed specifically for the different scales (local to global emissions, cities vs. industries, etc.) relevant for the users, and will also include impact of cross-calibration with other missions like Microcarb.

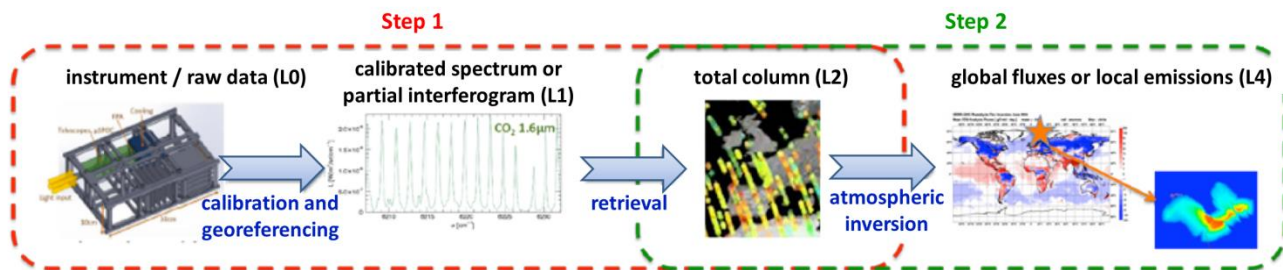


Figure 8. Level products. In GHG space missions, the target variable (surface fluxes, and in particular emissions – so-called L4 products) is not what is retrieved (total atmospheric columns XCO₂ – L2 products) from the observations (radiances – L1 products). A two-step approach is thus needed. First, after radiometric calibration, radiances measured by the instrument are interpreted in terms of total column, together with associated uncertainty and vertical sensitivity (which gives the contribution of each atmospheric layer to the total column). This step relies on an iterative loop between forward and inverse radiative transfer models. In a second step, the total columns are used to infer surface sources and sinks and their associated uncertainties through an atmospheric inversion, which usually relies on an atmospheric transport model.

The overall mission configuration will also be studied, with considerations about the space segment (payload, spacecraft, launcher) as well as the ground segment and communication architecture.

This descending analysis (from user needs to instrumental products) will be completed by an ascending analysis to establish a mission performance assessment. This will begin with the definition of various geophysical and instrumental scenarios. For each scenario, the aim is to develop a performance processing chain that will be used to characterise the

random and systematic errors and the vertical sensitivities associated to the retrieval of CO₂ total columns (including the aerosol data provided by the Spex instrument), and subsequently to assess their impact on the estimation of surface fluxes at global, regional and local scales.

3.2 Instrumental developments

As stated in Section 2, Nanocarb is still at an early stage. Works on Nanocarb will be led in four directions.

- Manufacturing and characterization of the interferometric plate¹⁹.
- Data calibration: the raw images may have to be radiometrically calibrated, but processing strategies have also to be defined to register the images (the co-addition of images thanks to the 2D field-of-view of Nanocarb is required to reach the target sensitivity on CO₂).
- Inversion of the partial interferograms, which will also allow to optimize the definition of the instruments, especially the OPD to be sampled.
- Definition of a performance model, including rule design and identification of sources of errors

Our goal is to have a prototype to be used for the airborne campaign (see next sub-section). Due to the tight delay of the project, it is likely that the full performance of the Nanocarb concept will not be reached with this prototype, but the point is to validate the coherence between the prototype and the performance model, and to identify risks or difficulties for a future space mission.

Another key instrument in the Scarbo concept is the aerosol sensor, since one of the main biases on GHG estimations comes from aerosols. The project will thus include the definition of the in-space support instrument to measure aerosols, a good starting point being SpexLite, a high performance at moderate cost aerosol space instrument⁷.

3.3 Airborne demonstration campaign

The Scarbo project includes an airborne campaign, the objectives of which being the followings.

- Validate the Nanocarb measurement principle.
- Assess the performances of the NanoCarb prototype performances by comparison with a reference sensor. This reference sensor is the Methane Airborne Mapper (Mamap⁸).
- Quantify the impact of aerosol scattering on GHG measurement with additional information on aerosol provided by SPEX.

4. CONCLUSION

Measuring sources, sinks, and fluxes of GHG from space is a key need for assessing the effectiveness of GHG emission reduction policies. The solution proposed by Scarbo is a constellation of small satellites dedicated to CO₂ and CH₄ monitoring. The scope of this 3-year project is not to go up to the achievement of the constellation, but to perform technical feasibility study and to assess mission needs and performance. An airborne campaign will allow to experimentally validate the technological developments, especially the Nanocarb instrument, which is at the heart of the Scarbo project. This instrument is a compact snapshot imaging interferometer, based on an array of low finesse Fabry-Perot filters. Due to the quasi-periodicity of the CO₂ spectrum around 1.6 μm , measuring only partial interferograms will allow to retrieve CO₂ concentration. Short-terms works are the manufacturing of the interferometric plate, and the development of the interferogram inversion chain.

ACKNOWLEDGEMENTS

Nanocarb initiated in the framework of the LabEx FOCUS ANR-11-LABX-0013.

Scarbo project has received funding from the European Union's H2020 research and innovation program under grant agreement No 769032.

REFERENCES

- [1] "About GoSat," www.gosat.nies.go.jp/en/about_1_goal.html
- [2] "Orbiting Carbon Observatory 2," <https://oco.jpl.nasa.gov/>
- [3] "GHGSat Surveillance globale des émissions," www.ghgsat.com/fr/
- [4] Pasternak, F., Bernard, P., Georges, L., and Pascal, V., "The Microcarb instrument," Proc. SPIE 10562, 105621P (2016)
- [5] Sierk, B., Löscher, A., Caron, J., Bézy, J.-L., and Meijer, Y., "CarbonSat instrument pre-developments : towards monitoring carbon dioxide and methane concentration from space," Proc. SPIE 10562, 105622C (2016)
- [6] Gousset, S., Le Coarer, E., Guérineau, N., Croizé, L., Laveille, T., and Ferrec, Y., " NANOCARB-21: a miniature Fourier-transform spectro-imaging concept for a daily monitoring of greenhouse gas concentration on the Earth surface," Proc. SPIE 10562, 105624U (2016)
- [7] Van Amerongen, A., Rietjens, J., Smit, M., Van Loon, D., Van Brug, H., Van Der Meulen, W., Esposito, M., and Hasekamp, O., "Spex the Dutch roadmap towards aerosol measurement from space," Proc. SPIE 10562, 105621O (2016)
- [8] Gerilowski, K., Tretner, A., Krings, T., Buchwitz, M., Bertagnolio, P. P., Belemezov, F., Erzinger, J., Burrows, J. P., and Bovensmann, H., " MAMAP – a new spectrometer system for column-averaged methane and carbon dioxide observations from aircraft: instrument description and performance analysis," Atmos. Meas. Tech. 4, 215-243 (2011)
- [9] Kyle, T.G., "Temperature soundings with partially scanned interferograms," Appl. Opt. 16(2), 326-333 (1977)
- [10] Fortunato, G., "Application of interferential correlation of spectrum to the detection of atmospheric pollutants," Journal of optics 9(5), 281-290 (1978)
- [11] Pierangelo, C., Hébert, P., Camy-Peyret, C., Clerboux, C., Coheur, P., Phulpin, T., Lavanant, L., Tremas, T., Henry, P., and Rosak, A., "SIFTI, a Static Infrared Fourier transform Interferometer dedicated to ozone and CO pollution monitoring," Proc. of 16th International TOVS Study Conferences (ITSC), 375-385 (2008)
- [12] Grieco, G., Masiello, G., and Serio, C., "Interferometric vs spectral IASI radiances: Effective data-reduction approaches for the satellite sounding of atmospheric thermodynamical parameters," Int. J. Remote Sens. 2(10), 2323-2346 (2010)
- [13] Gousset, S., Le Coarer, E., Barthélémy, M., Guérineau, N., Croizé, L., and Ferrec, Y., "Spectrométrie TF statique sur Nanosat pour l'observation de l'atmosphère," Journée Nano-Satellites et Photonique (Toulouse, France, 24th April 2017)
- [14] Gousset, S., Croizé, L., Le Coarer, E., Ferrec, Y., Brooker, L., and Scarbo consortium, "NanoCarb part 2: Performance assessment for total column CO2 monitoring from a nano-satellite," Proc. of International Conference on Space Optics ICSO2018 (2018)
- [15] Rommeluère, S., Guérineau, N., Deschamps, J., De Borniol, E., Million, A., Chamonal, J.-P., and Destefanis, G., "Microspectrometer on a chip (MICROSPOC) : first demonstration on a 320x240 LWIR HgCdTe focal plane array," Proc. SPIE 5406, 170-177 (2004)
- [16] Pisani, M., and Zucco, M., "Compact imaging spectrometer combining Fourier transform spectroscopy with a Fabry-Perot interferometer," Opt. Exp. 17(10), 8319-8331 (2009)
- [17] Lucey, P., and Akagi, J., "A Fabry-Perot Interferometer with a Spatially Variable Resonance Gap Employed as a Fourier Transform Spectrometer," Proc. SPIE 8048, 80480K (2011)
- [18] Mouzali, S., "Modélisation spectrale de détecteurs matriciels infrarouge HgCdTe: application à un micro-spectromètre," PhD Thesis, Université Paris-Saclay, (2015)
- [19] Ehrhardt, H, Gousset, S., Boussey, J., Panabière, M., Le Coarer, E., Croizé, L., Ferrec, Y., Brooker, L, and the Scarbo consortium, "Characterization by OCT of a new kind of micro-interferometric components for the Nanocarb miniature imaging spectrometer," Proc. of International Conference on Space Optics ICSO2018 (2018)